

H. GLUR✉  
A.N. KIRIEEV  
E. WYSS  
H.P. WEBER

# Systematic engineering of paraxial coherent fields with spherical optical systems

Institute of Applied Physics, University of Bern, Sidlerstrasse 5, 3012 Bern, Switzerland

Received: 1 February 2005 / Revised version: 4 April 2005  
Published online: 3 June 2005 • © Springer-Verlag 2005

**ABSTRACT** The concept of the Iwasawa decomposition [1] of  $ABCD$  ray-matrices is used for a systematic calculation of field distributions appearing in spherical optical systems. Examples of optimization for applications are calculated.

**PACS** 41.85.Ew; 42.15.Eq

## 1 Introduction

If the amplitude and phase of a light beam are known over its cross-section at one location, it allows one to calculate the field at any position. This article shows an efficient way to get systematically the possible field distributions in a spherical optical system for stigmatic, coherent and monochromatic beams. It allows the derivation of criteria for the optical system needed to come close to a desired field distribution. The method is applied for optimizing beam shaping (like e.g., in [2]) and the application of custom modes for material processing.

To calculate the second intensity moment  $\sigma$  and the phase-front curvature radius  $R$  the  $q$ -parameter formalism is well suited [3, 4]. The beam width  $\sigma$  and the curvature radius of the phase-front  $R$  can be described by the the complex  $q$ -parameter which transforms in an optical system as [4]

$$q_2 = \frac{Aq_1 + B}{Cq_1 + D}. \quad (1)$$

$A$ ,  $B$ ,  $C$  and  $D$  denote the ray-matrix elements and  $q$  is defined by the relation [3]

$$\frac{1}{q} = \frac{1}{R(z)} - i \frac{M^2}{2k\sigma^2(z)}. \quad (2)$$

$M^2$  corresponds to the beam propagation factor and  $z$  to the distance in the direction of propagation. The field distribution has to be calculated, e.g., by evaluating the Collins integral (3, 4) according to [5]. It is valid for beams propagating through optical elements that can be described by  $4 \times 4$  ray-matrices [5]. In our case the  $4 \times 4$  matrix can be reduced to a  $2 \times 2$  matrix due to rotational symmetry. To get the calculations more systematic and intuitive, the Iwasawa decomposition [1] of the  $2 \times 2$  ray-matrices is used. It has to be

mentioned that the validity of the Collins integral (3, 4) is limited to cases with no loss or gain in the optical system and where the Fresnel approximation of the Kirchhoff integral is valid.

## 2 Theory

The Collins integral can be written in the form [1]

$$u(x, y) = \frac{-i}{\lambda B} \exp\left(\frac{i\pi D}{\lambda B} r^2\right) \times \int \int \exp\left(-\frac{2\pi i}{\lambda B}(xx' + yy')\right) \times u'(x', y') \exp\left(\frac{i\pi A}{\lambda B} r'^2\right) dx' dy' \quad \text{if } B \neq 0 \quad (3)$$

$$u(x, y) = \frac{1}{A} \exp\left(\frac{i\pi C}{\lambda A} r^2\right) u'\left(\frac{x}{A}, \frac{y}{A}\right) \quad \text{if } B = 0 \quad (4)$$

where  $A$ ,  $B$ ,  $C$  and  $D$  are the beam propagation matrix elements and  $r^2 = x^2 + y^2$ . The calculation of the field distributions appearing in an optical system by means of the Collins integral (3, 4) can be done more systematically using the Iwasawa decomposition [1] of the  $ABCD$  matrices, which is schematically described in Fig. 1.

For stigmatic beams without loss of generality the elements  $B$  and  $C$  can be scaled with the Rayleigh range

$$z_0 = \frac{2k\sigma_0^2}{M^2} \quad (5)$$

to get a dimensionless  $AB'C'D$  matrix.<sup>1</sup>  $\sigma_0$  corresponds to the second intensity moment in the waist. How the corresponding parameters  $\sigma$ ,  $\sigma_0$ ,  $M^2$  and  $R$  can be calculated from a given field distribution is shown in [3]. From now on we use the dimensionless parameters

$$B' = \frac{B}{z_0}, \quad C' = Cz_0, \quad f' = \frac{f}{z_0}. \quad (6)$$

In the Iwasawa decomposition the only part of the matrix which can change the shape of the field is formally equivalent to a GRIN lens [6]. Mathematically this corresponds to a phase-space rotation or a fractional Fourier transformation.

<sup>1</sup>Of course the vector  $(x, \alpha)$  has to be transformed to  $(x/z_0, \alpha)$  and the  $q$ -parameter has also to be scaled with  $z_0$ .

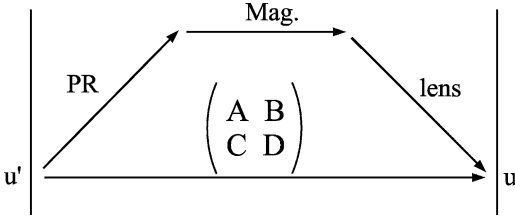


**FIGURE 1** Schematic description of the matrix decomposition. A phase-space rotation (PR) followed by a pseudo magnification (Mag.) and a lens are equivalent to the transformation via the  $ABCD$  matrix

The complete decomposition of the dimensionless matrix has the form

$$\begin{pmatrix} A & B' \\ C' & D \end{pmatrix} = \underbrace{\begin{pmatrix} 1 & 0 \\ -1/f' & 1 \end{pmatrix}}_{(\text{lens})} \underbrace{\begin{pmatrix} b & 0 \\ 0 & 1/b \end{pmatrix}}_{(\text{Mag.})} \underbrace{\begin{pmatrix} \cos \phi & \sin \phi \\ -\sin \phi & \cos \phi \end{pmatrix}}_{(\text{PR})}, \quad (7)$$

where (PR) corresponds to a phase-space rotation and (Mag.) represents a magnification which scales up positions and scales down angles by the same factor. The operation (PR) is the only one for which Eqs. (3) and (4) have to be evaluated. The other two parts can be calculated by Eq. (4). By evaluating the expression (2) and comparing the left and the right sides, one obtains

$$\begin{aligned} \phi &= \arctan\left(\frac{B'}{A}\right), \quad b = \sqrt{A^2 + B'^2}, \\ f' &= \frac{B'}{\frac{A}{A^2+B'^2} - D} = \frac{-A}{\frac{B'}{A^2+B'^2} + C'}. \end{aligned} \quad (8)$$

The phase-space angle  $\phi$ , which is a parameter of the shape of the propagating field, only depends on the matrix elements  $A$  and  $B'$  with the last parameter describing essentially the deviation from the perfect imaging plane. This fact can also be concluded directly by looking at the part inside the integral of expression (3). The decomposition can be comprehended in a more intuitive way. Every beam propagation matrix can be divided into three operations changing at least one of the properties like the relative intensity distribution, the beam width and the spherical curvature of the phase front. The first operation (PR) is the only one which is able to change the relative field distribution,<sup>2</sup> the second one (Mag.) only changes  $\sigma$  and the third one (lens) only changes  $R$ . If the field is starting in its waist, the operation (PR) does not change  $q$  ( $\sigma$  and  $R$ ).<sup>3</sup> The systematic field propagation through the phase-space allows the investigation of the possible field distributions that can be found in the whole optical systems. This feature can be even further generalized. The corresponding optical elements of the system can be found after optimization for the best shape of the field distribution for the given application.

<sup>2</sup>Since  $u$  is complex, it is valid for the intensity profile as well as for the non-spherical part of the phase-front.

<sup>3</sup>Without any loss of generality, we can assume the field to be in its waist. If the field is not in the waist, we can calculate the location of the waist and adapt the ray-matrix.

The phase-space rotations do not modify the shape of individual spherical modes. However it modifies the superposition of fields of individual modes. We consider in the following two types of superpositions with well defined amplitude and phase relation.

### 3 Examples

We concentrate on the influence of this phase angle only since the other operations are mathematically trivial.

#### 3.1 The in-phase super-mode of a three-core fiber

As a first example the electromagnetic field distribution of the in-phase super-mode of a strongly-coupled fiber laser array (ASM) is investigated. The generation of these super-modes is aimed to solve the power and the brightness up-scaling problem in fibers [7]. The calculated phase-space rotations of the ASM are shown in Fig. 2.

**3.1.1 Detecting intensity peaks.** A possible application is the systematic search of maximum intensity peaks in optical systems since it is important to know where and how large they are to avoid material damages. Figure 3 shows the relative magnitude of the maximum intensity peak compared to its near field value at different phase-space angles for the ASM.

Using relations (8) we obtain for the intensity peak relative to the original intensity peak in the optical system

$$\frac{I}{I_0} = \frac{I_{\text{rel}}(\phi)}{b^2} = \frac{I_{\text{rel}}(\arctan(\frac{B'}{A}))}{A^2 + B'^2}, \quad (9)$$

where  $I_0$  stands for the maximum initial intensity,  $I$  for the maximum local intensity and  $I_{\text{rel}}$  for the function plotted in Fig. 3. The maximum intensity peak with a fixed  $\sigma$  appears at  $\phi = 90^\circ$ . In a similar way e.g., the width of the 90% energy mark in the whole optical system can be calculated in a systematic way.

**3.1.2 Material processing.** Because at  $\phi = 90^\circ$  the field of the ASM is closest to radial symmetry, it is convenient to use this field distribution for material processing. Inserting into Eq. (8) leads to the condition  $A = 0$  for the ray-matrix. If additionally the field has to be in its waist,  $D$  has to be 0 as well. The simplest optical system that fulfills both conditions is the  $f - f$  image

$$\begin{pmatrix} 0 & f'_i \\ \frac{1}{f'_i} & 0 \end{pmatrix}, \quad (10)$$

where  $f'_i$  stands for the focal length of the imaging lens and corresponds to the parameter  $b$  in Eq. (7). Inserting the propagation matrix (10) into Eq. (2) leads to

$$f'_i = \frac{\sigma'_2}{\sigma'_1} \quad (11)$$

for the focal length of the imaging lens with an initial beam width  $\sigma'_1$  and the desired beam width  $\sigma'_2$ .

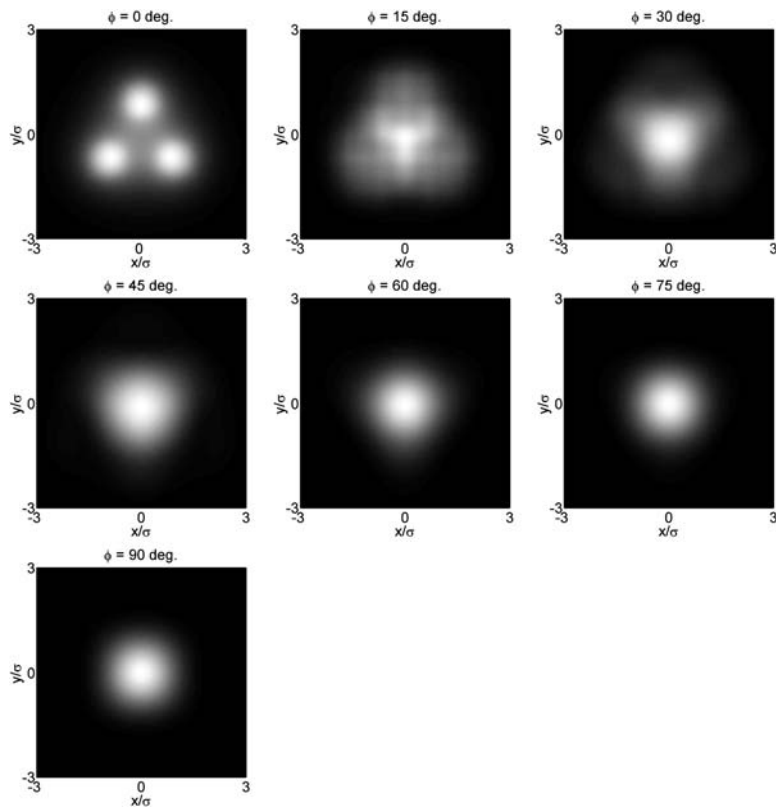


FIGURE 2 Intensity profiles of the ASM for different phase-space angles  $\phi$

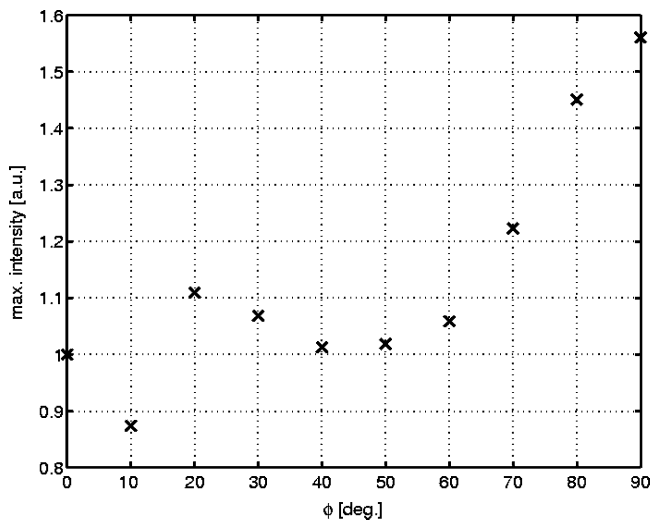


FIGURE 3 Maximum intensity peak of the ASM in the phase-space

### 3.2 The super-Gaussian beam

As second example the super-Gaussian field distribution is investigated as a practical approximation of the flat top profile which is desirable e.g., in second harmonic generation. We investigated the 12th order super-Gaussian mode (SGM) which is defined as

$$u(r) = u_0 \exp \left\{ - \left( \frac{r}{w_0} \right)^n \right\}, \quad (12)$$

where  $n = 12$  is the super-Gaussian index. Figure 4 shows the intensity profiles for the SGM for different phase-space angles  $\phi = 0^\circ$  or  $90^\circ$ .

## 4 Application

The theory described above can be applied to different problems. If we want to avoid non-spherical elements in a laser resonator with the three-core fiber the phase-space angle has to be  $\phi = 0^\circ$  or  $90^\circ$  since only there the field has no non-spherical aberrations.<sup>4</sup> We try to find the optimum resonator configuration for beam shaping. The deviation from the spherical phase-front only depends on  $\phi$  as shown in Fig. 5 for the SGM.

This deviation is most pronounced between  $\phi = 10^\circ - 30^\circ$ . Intuitively beam-shaping (like e.g., in [8]) is expected to be done the best in this region, since the phase-front distortion is strongest. A physically more meaningful crucial parameter is the energy theoretically needed to superpose to the field to reach a phase conjugation

$$\int dr \cdot r \cdot I(r) |e^{2i\theta(r)} - e^{2i\theta_0}|^2, \quad (13)$$

where  $I(r)$  stands for the intensity distribution,  $\theta(r)$  for the phase of the field and  $\theta_0$  for an arbitrary constant phase which underlies the condition

$$\frac{\partial}{\partial \theta_0} \int dr \cdot r \cdot I(r) |e^{2i\theta(r)} - e^{2i\theta_0}|^2 = 0. \quad (14)$$

<sup>4</sup>This does not automatically mean an  $f - f$  or a telescope image. Spherical mirrors are allowed.

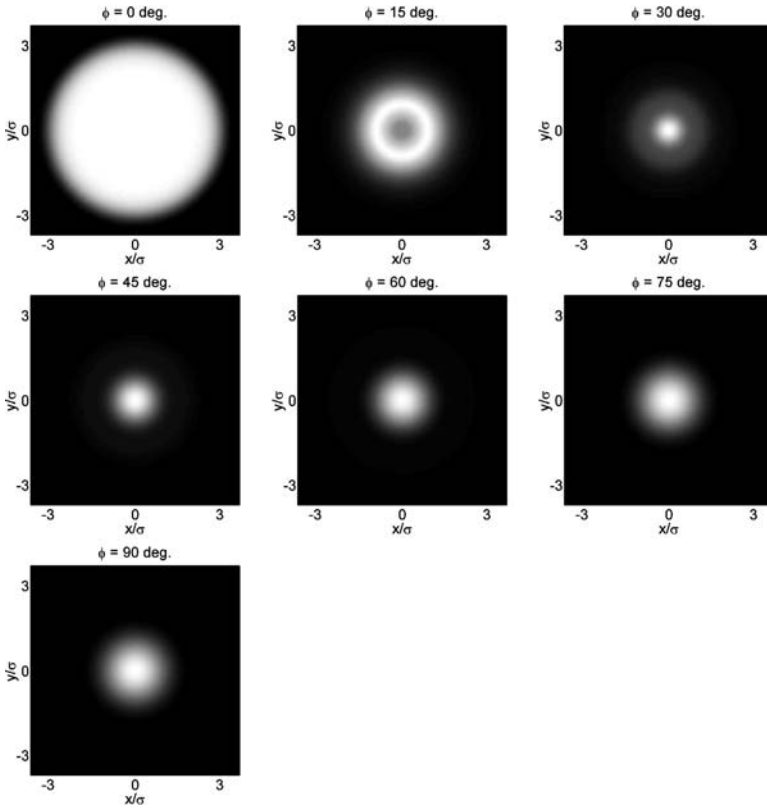


**FIGURE 4** Intensity profiles of the *SGM* for different phase-space angles  $\phi$

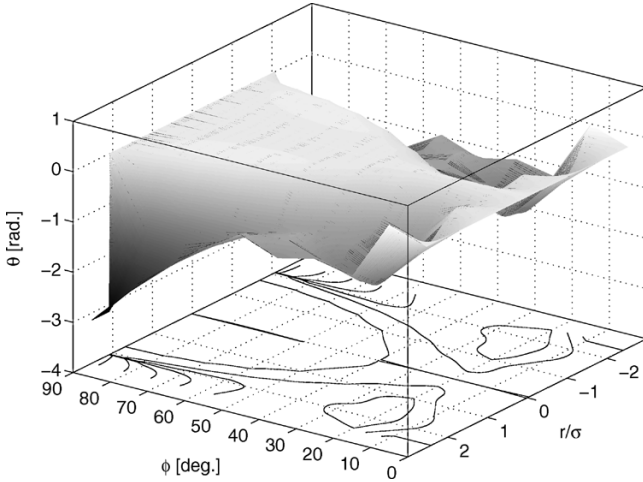


**FIGURE 5** Phase front of the *SGM* as a function of the phase-space rotation angle.

Evaluating condition (14) results in

$$\tan(2\theta_0) = \frac{\int dr \cdot r \cdot \sin(2\theta(r))I(r)}{\int dr \cdot r \cdot \cos(2\theta(r))I(r)}. \quad (15)$$

Evaluating Eq. (13) with  $\theta_0$  from Eq. (15) leads to Fig. 6. As expected this relative overlap intensity gets zero for  $\phi = 0^\circ$  and  $\phi = 90^\circ$  if the field has a plane phase-front at  $\phi = 0^\circ$ .

From Fig. 6, we can conclude that the optimum point to generate the *SGM* with a adaptive mirror would be at  $\phi \approx 25^\circ$  which quantitatively underlines the intuitive guess. It is most convenient to have the desired field distribution in its waist since in this case the theoretical maximum deformation the

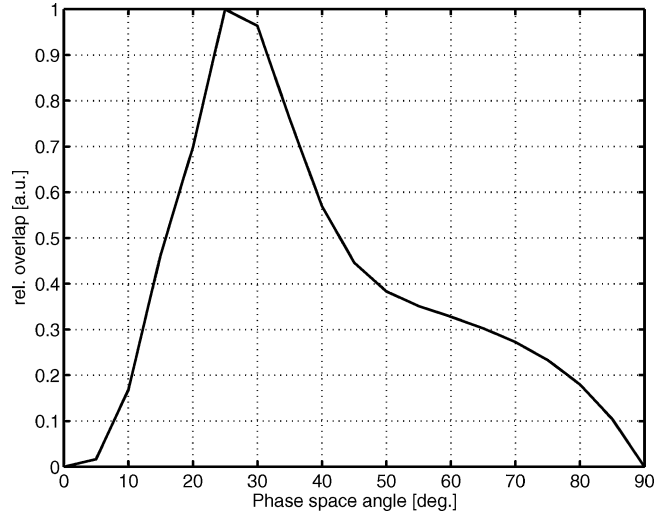


**FIGURE 6** Overlap between the phase front distortion and the intensity profile of the *SGM*

mirror has to manage is  $\lambda/2$ . The optimum scaling factor is a trade-off between exploiting the full resolution of the adaptive mirror and avoiding losses. It depends on the dimensions of the laser rod and the adaptive mirror and the transversal resolution of the adaptive mirror. The *ABCD* matrix is completely defined by these three conditions, and we have to think about a corresponding experimental setup. The ray-matrix can be obtained by inserting into Eq. (7) and gets

$$\begin{pmatrix} b \cos \phi & b \sin \phi \\ -\frac{\sin \phi}{b} & \frac{\cos \phi}{b} \end{pmatrix} \quad (16)$$

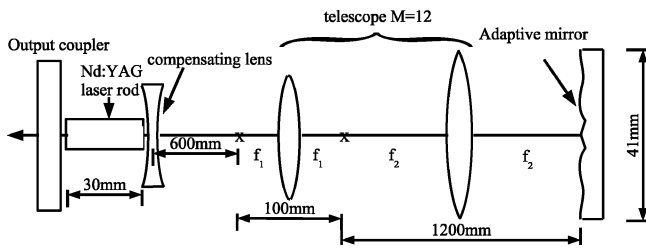


FIGURE 7 Setup for the generation of the SGM

The simplest way to get a well-defined phase-space angle  $\phi$  in the waist is to under-compensate the thermally induced lens of the Nd:YAG laser as shown in Fig. 7.

Then the resulting waist can be imaged with a telescope to the adaptive mirror. The ray-matrix before the telescope has approximately<sup>5</sup> the form

$$\begin{pmatrix} 1 - \frac{L'}{f'} & L' \\ -\frac{1}{f'} & 1 \end{pmatrix} \quad (17)$$

Inserting Eq. (17) into Eq. (16) leads to  $b = \cos \phi$ ,  $L' = \cos \phi \sin \phi$  and  $f' = \cot \phi$ . Inserting  $\phi = 25^\circ$  and assuming  $\sigma_0 \approx 0.5$  mm at the output coupler, we get  $z_0 \approx 1.65$  m and therefore  $f \approx 1.1$  m and  $L' \approx 0.63$  m. Note that  $f$  stands for the resulting net lens effect, not for the focal length of the compensating lens itself. The magnification factor of the intra-cavity telescope is chosen to be  $M = 12$ . These values lead to Fig. 7.

## 5 Conclusion

The Iwasawa decomposition of the  $ABCD$  matrix was shown to be an useful way to investigate the propagation of arbitrary coherent, monochromatic and stigmatic beams through spherical optical systems. It is based on the decomposition of the ray-matrix into a phase-space rotation, a magnification and a spherical lens transformation. Only the phase-space rotation provides information about the intensity distribution and the non-spherical part of the phase front of the propagating beam. The  $q$ -parameter formalism [3] has been applied for the calculation of the second intensity moment and the spherical part of the phase-front. As practical examples the method has been applied for the characterization of the in-phase super-mode of a fiber array and the optimization of a setup for the generation of a super-Gaussian mode with an adaptive mirror.

## REFERENCES

- 1 R. Simon, N. Mukunda, J. Opt. Soc. Am. A **15**, 8 (1998)
- 2 C. Paré, P.A. Bélanger, IEEE J. Quantum Electron. **30**, 4 (1994)
- 3 P.A. Bélanger, Opt. Lett. **16**, 4 (1991)
- 4 N. Hodgson, H. Weber, *Optical Resonators* (Springer-Verlag, London, 1997)
- 5 S.A. Collins, J. Opt. Soc. Am. **60**, 9 (1970)
- 6 L.M. Bernardo, Opt. Eng. **35**, 3 (1996)
- 7 A.N. Kireev, T. Graf, H.P. Weber (submitted for publication in J. Lightwave Technol)
- 8 M. Gerber, T. Graf, A. Kudryashov (submitted for publication in Appl. Phys. B)

<sup>5</sup>The distance from the output coupler to the compensating lens has to be significantly smaller than the focal length of the thermal lens and the distance to the telescope.